doi: 10.5028/jatm.2012.04044912

# Wind Tunnel Simulation of the Atmospheric Boundary Layer for Studying the Wind Pattern at *Centro de Lançamento de Alcântara*

**Ana Cristina Avelar[1]*, Fabrício Lamosa Carneiro Brasileiro[2], Adolfo Gomes Marto[1], Edson R. Marciotto[1], Gilberto Fisch[1], Amanda Fellipe Faria[1]**

[1]Instituto de Aeronáutica e Espaço – São José dos Campos/SP – Brazil

[2]Universidade Paulista – São José dos Campos/SP – Brazil

***Abstract:*** *Centro de Lançamento de Alcântara is the main Brazilian launching center. In spite of presenting several desirable aspects, due to its proximity to the Equator, it has a peculiar topography because of the existence of a coastal cliff, which modifies the characteristics of the atmospheric boundary layer. This may affect rocket-launching operations, especially when associated with safety procedures. This work is a continuation of previous experimental studies about the airflow pattern at this launching center. An improved way of simulating the atmospheric boundary layer in a short-test section wind tunnel using passive methods is presented here. It is also presented a preliminary analysis of the airflow pattern in Centro de Lançamento de Alcântara, at specific positions as the edge of cliff and around the mobile integration tower, from wind tunnel measurements using particle image velocimetry. Three values of Reynolds number, based on the coastal cliff height, l, ranging from 6.8×105 to 2.0×106, were considered.*

***Keywords:*** *Atmospheric Flow, Wind Tunnel, Boundary Layer, Centro de Lançamento de Alcântara.*

## LIST OF SYMBOLS AND NOMENCLATURES

| | |
|---|---|
| $\alpha$ | Power law equation coefficient |
| CLA | *Centro de Lançamento de Alcântara* |
| ABL | Atmospheric Boundary Layer |
| $\delta$ | Boundary layer thickness |
| $H$ | Wind tunnel height |
| IBL | Internal boundary layer |
| $I_u$ | Turbulence intensity |
| $l$ | Coastal cliff height |
| MIT | Mobile integration tower |
| PIV | Particle image velocimetry |
| TA-2 | Aeronautic Wind Tunnel of Institute of Aeronautics and Space |
| $u(z)$ | *L*ogarithmic velocity profile |
| $U(z), U(z_r)$ | Mean velocities corresponding to heights $z$ and $z_r$ |
| $U_{inf}$ | *F*ree stream velocity |
| $u_*$ | Friction velocity |
| $z_r$ | Reference height |
| $W$ | Wind tunnel width |

Received: 04/09/12 Accepted: 10/10/12

*author for correspondence: anacristina.avelar@gmail.com

Praça Marechal Eduardo Gomes, 50 – Vila das Acácias

CEP 12228-904 – São José dos Campos/SP – Brazil

## INTRODUCTION

The majority of the Brazilian rockets are launched from the *Centro de Lançamento de Alcântara* (CLA), which has a privileged geographical location, 2º 18'S that enables the operation of suborbital vehicles and satellites with safety launchings in several directions over the Atlantic Ocean (Pires *et al.*, 2008; Avelar *et al.*, 2010; Fisch *et al.*, 2010, Pires *et al.* 2010). An effective use of the launch opportunities at CLA is possible due to the climate conditions with a well-defined rain regime and winds of tolerable intensity, and no significant temperature variations. In addition, low demographical density allows the displacement of several sites for launching or logistic support. However, despite the many favorable aspects, mainly because of its proximity to the Equator, the launching center has a peculiar topography due to the existence of a coastal cliff with 40m height (Fig. 1), which can modify the atmospheric boundary layer (ABL) characteristics and consequently affect the safety of rocket launching operations, since the rockets launching pad and the place where the space vehicles are assembled, i.e., mobile integration tower (MIT), are located around 150 to 200m from the border, respectively. Another important physical feature occurrence at the CLA is the formation of an internal boundary layer (IBL) as a consequence of the surface

roughness variation, from ocean surface to continental terrain. The wind blowing from the oceanic smooth surface interacts with the low woodland vegetation modifying itself with the formation of an IBL (Pires, 2009), which makes the study of the meteorological conditions and wind flow pattern in this region even more important.

Figure 1. A general view of *Centro de Lançamento de Alcântara.*

The simulation of an ABL in a wind tunnel with short-test section is quite complicated and there are several methods for this purpose discussed in the literature (Counihan, 1969). A simple way of generating thick boundary layers is by using passive methods (Barbosa *et al.*, 2002; Loredo-Souza *et al.*, 2004), in which the flow is forced to pass through a combination of spires, wedges or grids together with roughness elements distributed on the wall. Ten possible ways of simulating neutral, stable, and unstable atmospheric conditions in different wind tunnel types were described in Hunt and Fernholz (1975). A short review of the techniques used to thicken the boundary layer was presented by Barbosa *et al.* (2002). Besides, thickening devices with sophisticated geometry were described by Ligrani *et al.* (1979 and 1983). Unluckily, these methods are not straightforward from a fluid mechanics point of view to allow simplified and affordable designs, which have motivated researchers to choose satisfactory geometries by trial and error.

ABL physics is very complex, and the main reason for this complexity is the interaction between the airflow and the surface, which occurs primarily through mechanical and thermal mechanisms. The mechanical interaction arises from the friction caused by the wind against the ground surface, which causes the wind to be sheared, creating a wind profile and associated turbulence. In the absence of thermal process, the ABL is said to be neutral, and a logarithmic velocity profile *u(z)*, characterized by the friction velocity $u_*$ and the terrain roughness height $z_o$, is expected to be found (Loredo-Souza *et al.*, 2004). According to Barbosa *et al.* (2000), for wind speeds higher than 10m/s, the turbulence produced by the flow shear is much greater than that produced by the buoyancy, therefore thermal effects become negligible. This is the case of CLA, where strong winds are observed during the dry season, from July to December. The ABL and atmospheric flow pattern in the CLA region has already been studied from observations, numerical simulations, and wind tunnel measurements (Pires *et al.*, 2008; Avelar *et al.*, 2010; Fisch *et al.*, 2010; Marciotto *et al.*, 2012)

The present work is an extended version of a paper recently presented at the fourth AIAA Atmospheric and Space Environments Conference, in New Orleans, from 25 to 28 June 2012, Avelar *et al.* (2012), and it is also a continuation of a previous study (Avelar *et al.*, 2010), in which the procedures for a boundary layer simulation in a short-test section wind tunnel (TA-2) were described and some preliminary results of flow measurements using the particle image velocimetry (PIV) technique, with a simplified topography model of the CLA region, were presented.

Herein, the ABL was simulated using a combination of spires, barrier, and bottom wall surface roughness. The results confirmed the possibility of creating an ABL in the aeronautic wind tunnel, TA-2, of the *Instituto de Aeronáutica e Espaço*, in Brazil, without using screens downstream of the spires, as in a previous work (Avelar *et al.*, 2010). Three values of Reynolds number ($Re_l$) based on the coastal cliff height, $l$, ranging from $6.8\times10^5$ to $2.0\times10^6$ were considered. The purpose of investigating the influence of this flow parameter was to verify if the flow pattern, mainly behind the TMI, is sensitive to small Reynolds number variations. In addition, turbulence measurements from hot-wire techniques have been conducted. Some stereo PIV velocity measurements for the values of Reynolds number considered were also conducted, showing strong recirculation regions behind the TMI, and it was verified that the wind flow pattern is not very sensitive to small variations of this parameter.

## METHODOLOGY

### Wind velocity profiles

Empirical laws can be used to represent the wind profile inside the ABL, for example, the logarithmic and power law equations (Arya, 2001). According to the logarithmic law,

the vertical variation of the horizontal wind velocity, $U$, from the surface up to 100 to 150 m, which corresponds to the superficial boundary layer, may be represented by Eq. 1,

$$U(z) = \left(\frac{u_*}{k}\right) \ln\left(\frac{z_r}{z_0}\right) \quad (1)$$

where,

$u_*$: is the friction velocity,

$k$: is the Von Kármán constant,

$z_0$: is the mean terrain roughness, and

$z_r$: is assumed to be 10m, which is the height suggested by the World Meteorology Organization to represent the horizontal wind surface.

The friction velocity, $u_*$, is dependent on the wall shear stress, $\tau_w$, consequently being a measure of the logarithmic declivity close to the wall (Loredo-Souza *et al.*, 2004). Such equation has a better approximation of the wind profile close to the surface, however it is extensively employed also in the surface layer up to about 100m above sea level (Garratt, 1994).

The power law equation can be defined by Eq. 2,

$$\frac{U(z)}{U(z_{ref})} = \left(\frac{z_r}{z_{ref}}\right)^{\alpha} \quad (2)$$

where,

$U(z_{ref})$: is the mean velocity correspondent to a reference height $z_{ref}$.

The exponent $\alpha$ is a characteristic of the type of terrain. It varies from 0.11 for smooth surface as lakes and the ocean to 0.34 for cities with high density of buildings. For the ocean surface, some studies consider $\alpha$ between 0.11 (Hsu *et al.*, 1994; Barbosa *et al.*, 2002) and 0.15 (Blessmann, 1973).

Although commonly used, the power law equation has some drawbacks, which were pointed out by Loredo-Souza *et al.* (2004). Since this equation is valid for any value of $z_r$, the top of the ABL is not recognized in this model. The second issue is that in spite of providing a good representation of the mean velocity profile, this approach does not have a theoretical justification. Finally, the power law equation has a good adjustment in Ekman's layer, but not into the surface layer.

In the present work, the power law equation was used instead of the logarithmic one because of the difficulties in obtaining $z_0$ and $u_*$. In fact, according to Hsu (1988), *in situ* measurements of the aerodynamic roughness length are not always possible since it is related to both the wind speed and the wave characteristics of the ocean. The value of 0.11 for the exponent $\alpha$ was assumed in the power law equation.

## Wind tunnel atmospheric boundary layer modeling

The experiments were conducted in TA-2, which is a closed-circuit aeronautic subsonic wind tunnel. Its test section has a 2.10m height, $H$, and 3.00m width, $W$. A 1,600 HP motor produces a maximum speed of 120m/s through the test section. Spires, roughness elements, and a barrier positioned downstream of spires were used for simulation of a thick boundary layer. The spires consist of triangular steel plates fixed at the test section entrance. The combination of these elements generates the boundary layer profile in the section test. The spire dimensions depend on the desired boundary layer characteristics and on the wind tunnel size, and they were calculated following the methodology proposed by Blessmann (1973).

For the boundary layer formation, initially, a set of 180 small blocks with 80×80×20mm was displaced on the wind tunnel bottom wall separated by 150mm. A 200mm high barrier was positioned 350mm downstream of the spires. Nevertheless, different configurations obtained by removing the barrier and spires, or changing the density of the roughness elements were tried as well. Two multi-manometers, with Pitot tubes for dynamic pressure measurements installed along its height (Fig. 2), were used for monitoring the velocity profiles in the boundary layer. The tallest multi-manometer (rake 1) has 15 Pitot tubes equally distributed along its extension and spaced by 13mm. The smallest one (rake 2) has 16 Pitot tubes. The 11 lowest Pitot tubes are spaced by 5mm and the five highest ones, by 10mm. For each configuration, the ABL velocity profile was compared with a power law profile with

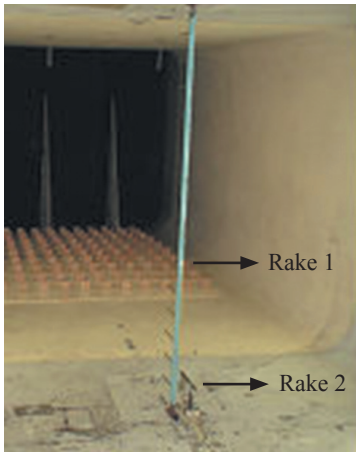


Figure 2. Multi-manometer with Pitot tubes.

$a$=0.11, which was assumed to be the closest of what is found over the ocean (Hsu *et al.*, 1994).

The positions where dynamic pressure measurements were carried out are represented in Fig. 3.

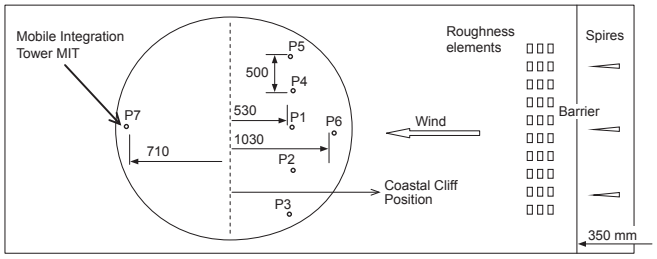


Figure 3. Positions in test section in which dynamic pressures values were measured with the multi-manometer.

The circle in Fig. 3 is located in the middle of the test section. The distance between the spires and wind tunnel central line was of 7,860mm.

**Turbulence measurements**

Turbulence measurements were performed for the free-stream velocity of, approximately, 40m/s. Mean velocity profiles and turbulence intensity levels were obtained using a constant temperature hot-wire anemometer, from Dantec Dynamics. These measurements were conducted only in the middle of the wind tunnel test section, in the location indicated as P1 in Fig. 3, after the simulation of the atmospheric boundary layer. It was used a straight golden-plated wire probe (55P01). For data collection, a sample rate of 10kHz was used. The measurements were conducted in several vertical positions. A manually controlled device (Fig. 4), which allowed the vertical displacement of the hot-wire probe during the experiment, was also used. Because of a physical limitation of this device, the highest vertical position where turbulence measurements were conducted was 765mm.

Figure 4. Hot-wire probe in the TA-2 test section.

**Particle Image Velocimetry measurements**

After the ABL simulation, a simplified model of the CLA topography was installed in the TA-2 test section, and PIV measurements were conducted at the edge of the coastal cliff and around the MIT. In the present study, the coastal cliff slope angle was assumed as 70º with the horizontal plane, and this value was then reproduced in the model. However, since this inclination angle is not constant along the coastal cliff length, as a continuation of the present analysis, other inclinations will be further considered.

The mean flow velocity was measured using a Dantec Dynamics two-dimensional PIV system (Fig. 5). The system was a double-cavity pulsed laser, Nd:Yag, 15Hz, with an output power of 200mJ per pulse at the wavelength of 532 nm (New Wave Research, Inc.) and two HiSense 4M CCD camera, built by Hamamatsu Photonics, Inc. with acquisition rate of 11Hz, spatial resolution of 2048×2048 pixels, and 7.4μm pixel pitch. A Nikon f# 2.8 lenses with 105mm of focal length was used. The laser sheet was shot from the wind tunnel top wall, which was replaced by a glass window, and such sheet was produced using cylindrical lens placed at the end of an articulated optical arm, which transmits the laser from its source to the region of focus (ROF). This arm was used to allow the laser sheet displacement over the model. The red circles in Fig. 5 indicate locations where PIV measurements were conducted, at the edge of the cliff and around the TMI.

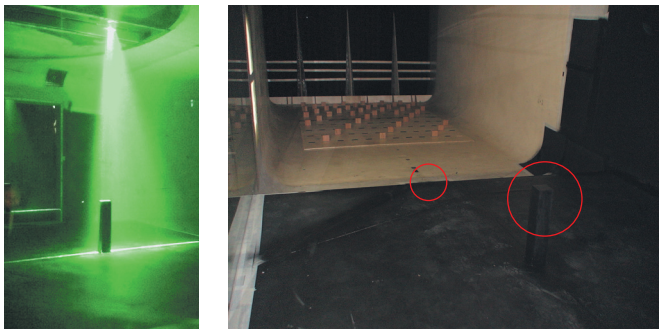

Figure 5. Particle image velocimetry measurements.

The flow was seeded with theatrical fog (polyethylene glycol water-solution) generated by a Rosco Fog Generator placed inside the wind tunnel diffuser. The digital camera was mounted on a Dantec Scheimpflug Camera Mounts fixed

on an aluminum trail supported by a three-axis-positioning device. The number of image pairs captured per second was 5.6, and around 200 image pairs, from each camera, were averaged for one measurement condition. The instantaneous images were processed using the adaptive correlation option of the commercial software Dynamic Studio, developed by Dantec Dynamics. A 32×32-pixel interrogation window with 50% overlap and moving average validation was used. The model was built in wood and painted in flat black to minimize laser reflections.

## RESULTS AND DISCUSSION

### Boundary layer velocity profiles

The configurations tested for the boundary layer generations and the velocity profiles obtained are presented in Figs. 6 to 21. The first three configurations, removing the spires, the barrier and the roughness elements were only tested to illustrate the role of these devices for an appropriated boundary layer profile simulation.

As can be noticed from Figs. 6 to 10, the spires have a major role in defining the boundary layer profile. However, without the roughness element, the generation of a thick boundary layer is not possible. The barrier has the purpose of generating a deficit of momentum in the level of the floor, contributing for the velocity profile adjustment close to the bottom surface.

Figure 13 presents the velocity profile obtained for configuration IV, in which the barrier, the spires, and all the 180 wood blocks were used. These results seem to indicate that an enhancement in the momentum deficit was necessary. With this purpose, wood strips perpendicularly to the spires were added, as shown in Fig. 14.

By adding the three horizontal strips, as observed in Fig. 15, the velocity profile is closer to the power law profile with the exponent 0.11.

Comparing Fig. 15 and 17 and observing the correspondent velocity profiles, it can be observed that modifying the

Figure 6. Configuration I – barrier and roughness elements.

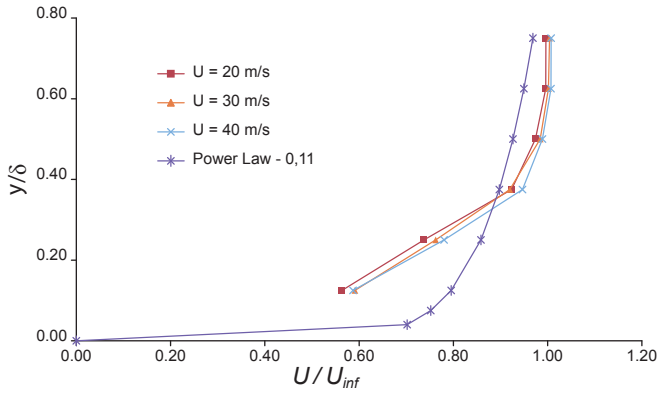


Figure 7. Velocity profiles for configuration I.

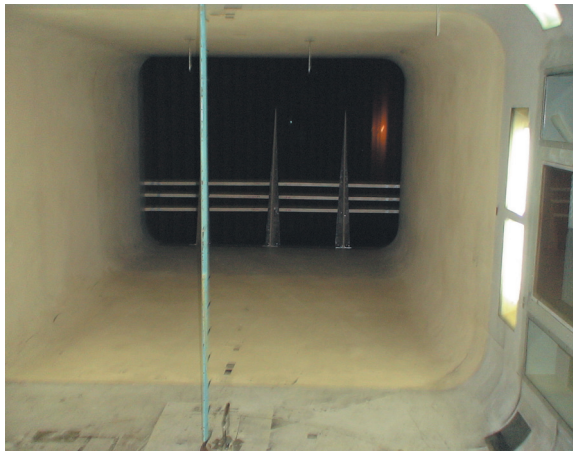

Figure 8. Configuration II – spires and horizontal strips.

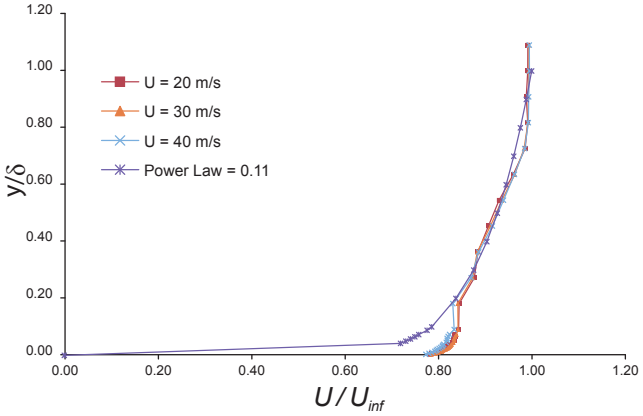


Figure 9. Velocity profiles for configuration II.

Figure 10. Configuration III – spires and roughness elements.

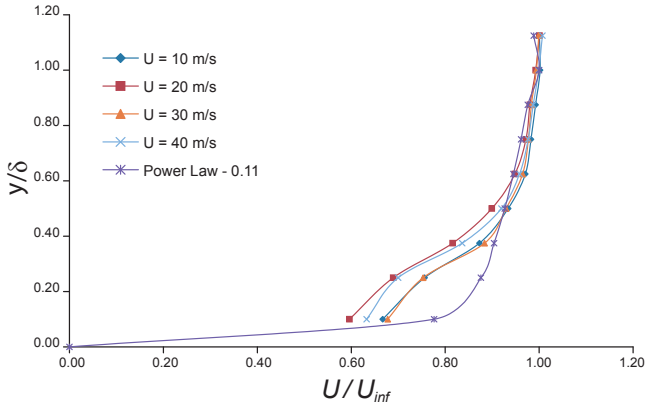


Figure 11. Velocity profiles for configuration III.

Figure 12. Configuration IV – spires, barrier, and roughness elements.

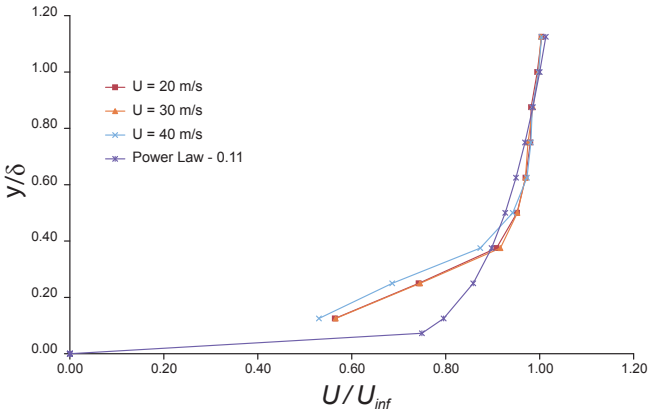


Figure 13. Velocity profiles for configuration IV.

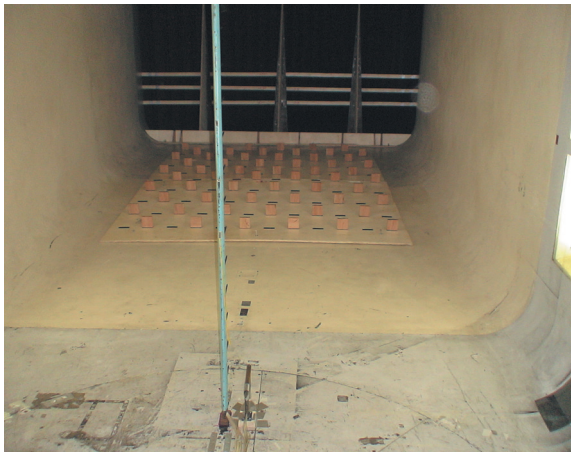

Figure 14. Configuration V – barrier and roughness elements.

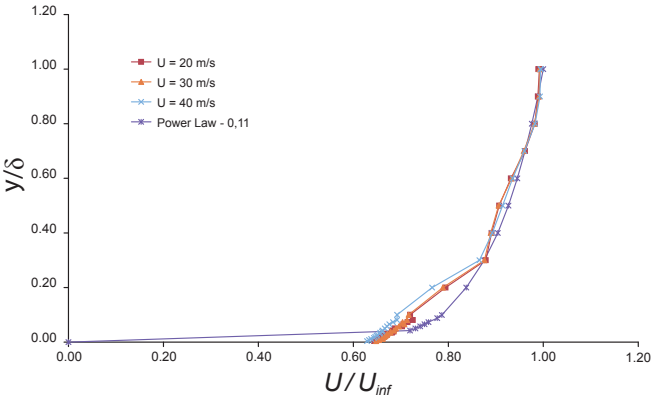


Figure 15. Velocity profiles for configuration V.

roughness element density, a fine adjustment in the boundary layer profile can be obtained.

Figures 18 to 21 were included to show some velocity profiles in different possitions in TA-2 test section. Fig. 19 shows that the wind tunnel lateral walls do not affect significatively the boundary layer velocity profile.

Figure 22 shows the configuration used in a previous study, Avelar *et. al*, 2010, for the boundary layer formation in the same wind tunnel, and Fig. 23 presents the velocity profile obtained.

Figure 16. Configuration VI – barrier, roughness elements, and strips.

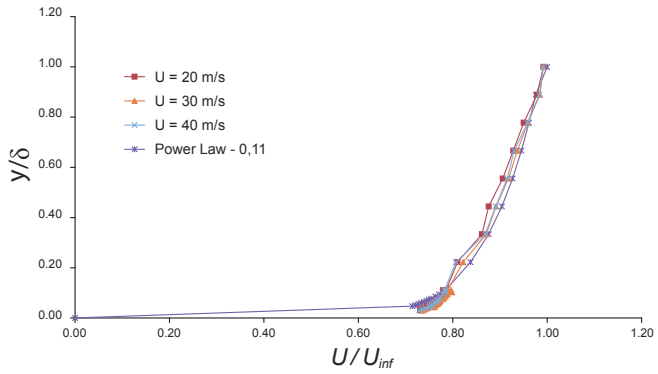


Figure 17. Velocity profiles for configuration VI.

Figure 18. Configuration VII – barrier, roughness elements, and strips. Measurement close to the lateral wall of the wind tunnel.

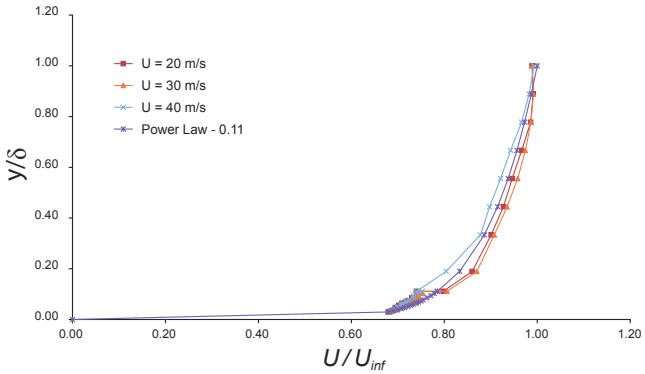


Figure 19. Velocity profiles for configuration VII.

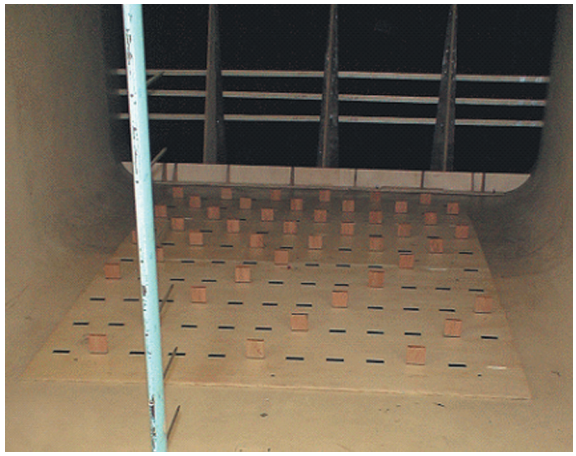

Figure 20. Configuration VIII – barrier, roughness elements, and strips. Measurement close to the mobile integration tower site.

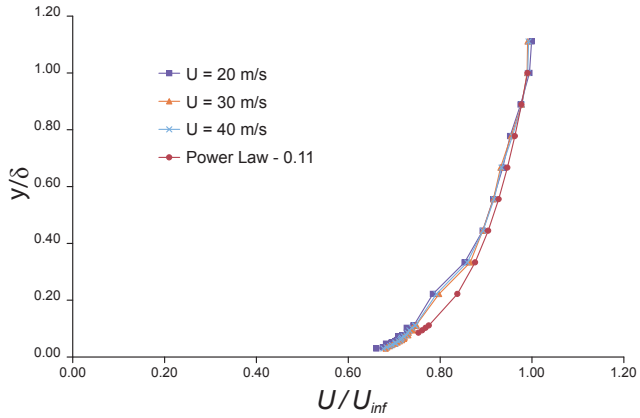


Figure 21. Velocity profiles for configuration VIII.

It can be observed that whenever the power-law is well followed, the dimensionless wind speed profiles collapse to a single curve, showing that there is no flow regime change for the range of speed studied (from 20 to 40m/s).

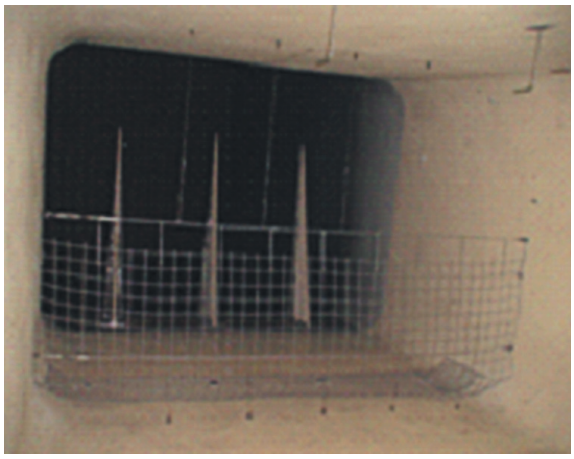

Figure 22. Configuration used in Avelar *et al.* (2010).

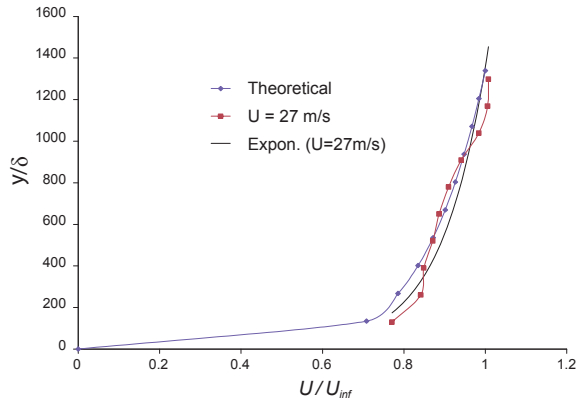


Figure 23. Velocity profiles from Fig. 21.

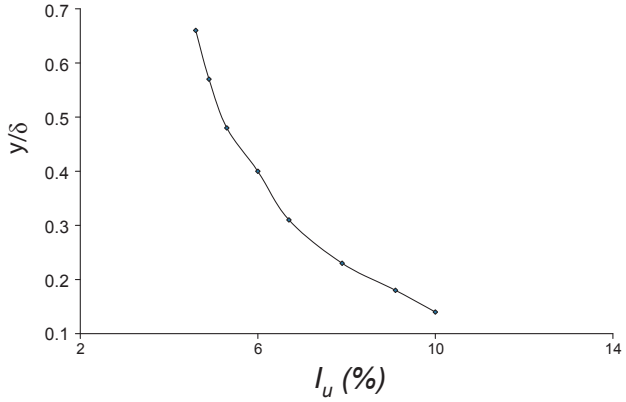


Figure 24. Turbulence profile in TA-2 test section – location P1.

## Turbulence measurement results

Table 1 shows the intensity turbulence, $I_u$, measured for various vertical positions and associated h/$\delta$ ratio in the central position of the TA-2 test section, where $h$ is the distance from the wind tunnel floor. These turbulence measurements were taken for the wind tunnel velocity of 40m/s. The turbulence measurements were conducted for the configuration shown in Fig. 20.

The turbulence profile correspondent to the values presented in Table 1 is presented in Fig. 24.

Table 1. Turbulence intensity measurements.

| Measurement position | $y$ (mm) | $I_u$ (%) | $y/\delta$ |
|---|---|---|---|
| P1 | 765 | 4.6 | 0.66 |
| P2 | 665 | 4.9 | 0.57 |
| P3 | 565 | 5.3 | 0.48 |
| P4 | 465 | 6.1 | 0.40 |
| P5 | 365 | 6.7 | 0.31 |
| P6 | 315 | 7.9 | 0.23 |
| P8 | 215 | 9.1 | 0.18 |
| P9 | 165 | 10.0 | 0.14 |

The turbulence intensity values measured in the generated boundary layer, represented in Fig. 24, are in agreement with the values encountered by Wittwer *et al.* (2012), who experimentally studied CLA small scale models, 1:400 in the wind tunnel "Joaquim Blessmann" of the laboratory *LAC/UFRGS,* in Porto Alegre, Brazil. In this study, mean and unsteady flow characteristics were evaluated using the hot-wire anemometer technique.

From Table 1 and Fig. 24, it can be observed that the turbulence profile has an expected behavior, with high turbulence intensity close to the wind tunnel floor. The frequency spectrums, for each vertical position where turbulence measurement were conducted, are shown in Fig. 25.

From Fig. 25, it can be observed that in the inertial range the -5/3 Kolmogorov's law is followed by all curves.

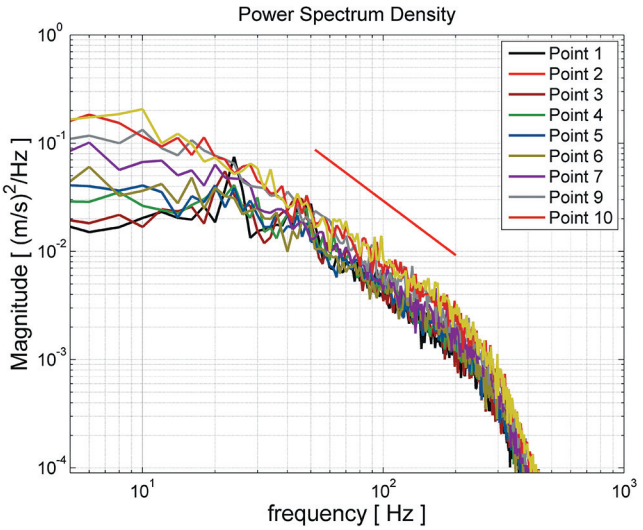


Figure 25. Turbulence spectrum for P1 to P10.

**Particle Image Velocimetry results**

A schematic representation of the CLA wind tunnel model is shown in Fig. 26. The squares numbers 1 and 2 indicate the positions over the model surface, in which the PIV measurements were carried out. In Fig. 27, PIV velocity flow maps are presented for the cliff slope of 70º and wind incidence direction of 0º.


Figure 26. Schematic representation of the *Centro de Lançamento de Âlcantara* physical model.

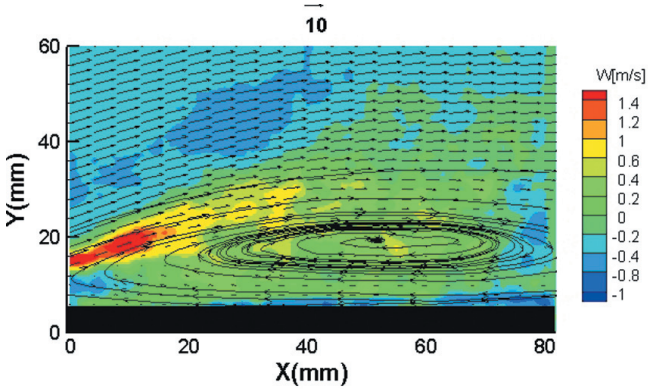


(a) $Re_l$ =6.8x10$^5$

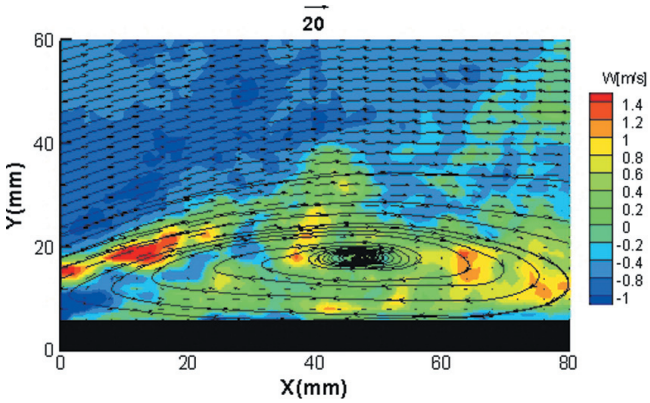


(b) $Re_l$ =1.4x10$^6$

Figure 27. Particle image velocimetry results for the edge of cliff, square number 1, for different $Re_l$ values.

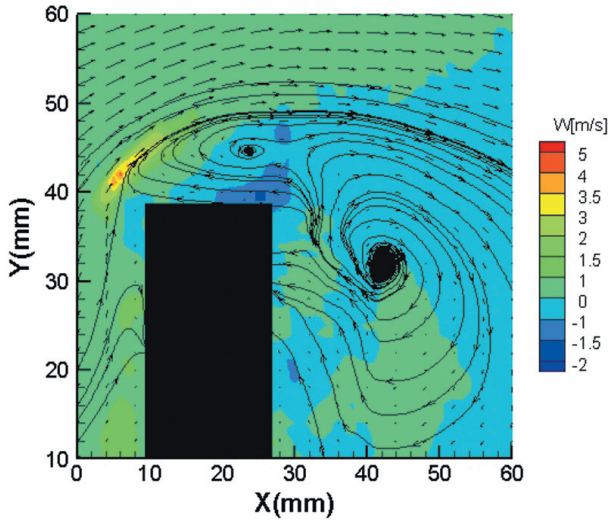


(a) $Re_l$ =6.8×10$^5$

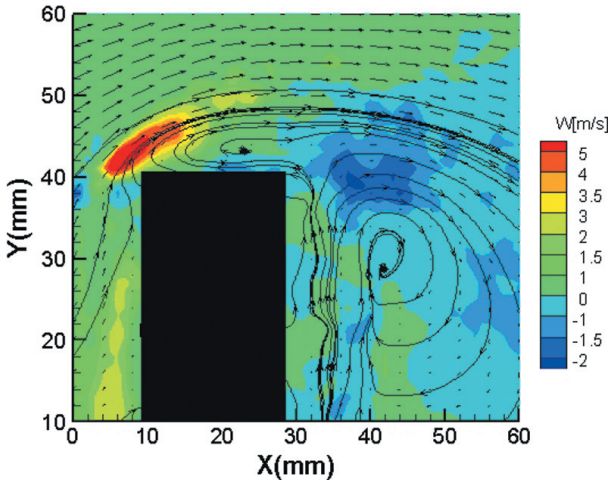


(b) $Re_l$ =1.4×10$^6$

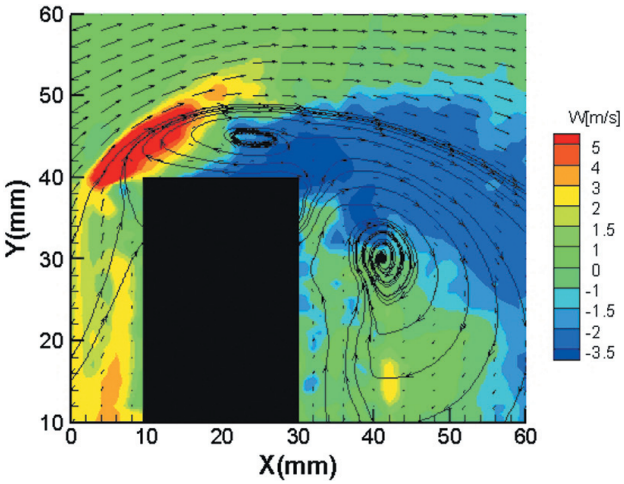


(c) $Re_l$ =2.0×10$^6$

Figure 28. Particle image velocimetry results around the mobile integration tower for different $Re_l$ values.

The PIV measurements were carried out with the purpose of investigating the influence of small variation of Reynolds number in the simulated flow pattern, and also to get insights about the three-dimensional behavior of the flow in CLA region. From Figs. 27 and 28, it can be observed an acceleration of the flow in the edge of the cliff and also in MIT first corner. However, as the flows in these regions are already separated, the Reynolds number seems not to play an important role. In fact, according to Larose and D'Auteuil (2006), it is expected that bluff bodies with sharp edges, which is the case of MTI, the aerodynamics characteristics are almost insensitive to Reynolds Number as long as this parameter reaches 10,000. It can be pointed out also that the IBL seems to grow asymptotically.

## CONCLUSIONS

Following a previous study on the simulation of the ABL in a short-test section wind tunnel, a combination of passive turbulence generators were tested in the present work. Good agreement between the boundary layer velocity profiles generated and the power law profile was observed when horizontal strips were added perpendicularly to the spires in the conventional setup (roughness, barrier, and spires). Whenever the power-law is well-followed, the dimensionless wind speed profiles collapse to a single curve, showing that there is no flow regime change for the range of speed studied (from 20 to 40m/s).

PIV measurements provided the vector velocity field around the step corner, representing the coastal cliff, and around the MIT. For the range of Reynolds number tested, no significant variations were observed on the circulation pattern. In both cases, a very turbulent wake was downstream observed. A future analysis of this research will compare wind tunnel simulation with actual flow observations.

## ACKNOWLEDGMENTS

The authors would like to thank the technicians José Rogério Banhara and José Ricardo Carvalho de Oliveira, the Engineers Alfredo Canhoto, Wellington dos Santos and Matsuo Chisaki, Ana Clara Dias Barbosa and Tailine Corrêa for their valuable help to this research. Also, to the *Agência Espacial Brasileira* (AEB), the *Conselho Nacional de Desenvolvimento Científico e Tecnológico* (CNPq) under the Grants 559949/2010-3, PQ 303720/2010-7 (Fisch), Universal 471143/2011-1 (Marciotto), and the *Fundação de Amparo à Pesquisa do Estado de São Paulo* (2010/16510-0) for their financial support.

## REFERENCES

Arya, S.P., 2001, "Introduction to Micrometeorology", Academic Press, USA, 2001, 2nd edition.

Avelar, A.C. *et al.*, 2012, "Atmospheric Boundary Layer Simulation in a Wind Tunnel for Analysis of the Wind Flow at the Centro de Lançamentode Alcântara", 4th AIAA Atmospheric and Space Environments Conference 25-28, New Orleans, Louisiana, AIAA paper 2012-2930.

Avelar, A.C. *et al.*, 2010, "Simulation of the Atmospheric Boundary Layer in a Closed Circuit Wind Tunnel with Short Test Section", 27th AIAA Aerodynamic Measurement Tecnology and Ground Testing Conference, Chicago, AIAA paper AIAA-2010-4343.

Barbosa, P.H.A. *et al.*, 2000, "Simulation of atmospheric boundary layer flows in short wind tunnels", Proceedings of do XI CBMET 2000, Rio de Janeiro, Brazil.

Barbosa, P.H.A. *et al.*, 2002, "Wind Tunnel Simulation of Atmospheric Boundary Layer Flows", Journal of the Brazilian Society of Mechanical Sciences, Vol. 24, No. 3, pp. 177-185.

Blessmann, J., 1973, "Simulação da estrutura do vento natural em um túnel de vento aerodinâmico", Tese (Doutor em Ciências), Instituto Tecnológico da Aeronaútica – ITA, São José dos Campos, Brazil, 169 p.

Counihan, J., 1969, "An improved method of simulating an atmospheric boundary layer in a wind tunnel", Atmospheric Environment, Vol. 3, pp. 197-214.

Fisch, G. *et al.*, 2010, "The Internal Boundary Layer at the Alcântara Space Center: Winds Measurements, Wind Tunnel Experiments and Numeric Simulations," Proceedings of the Fifth International Symposium on Computational Wind Engineering (CWE2010) Chapel Hill, North Carolina, USA May 23-27.

Garratt, J.R., 1994, "The Atmospheric Boundary Layer", Cambridge University Press, Cambridge, USA, 316 p.

H'su, S.A., 1988, "Coastal Meteorology", Academic Press, San Diego, 260 p.

Hsu, A.S. *et al.*, 1994, "Determining the Power-Law Wind-Profile Exponent under Near-Neutral Stability Conditions at Sea", Journal of Applied Meteorology, Vol. 33, No. 6, pp. 757-765.

Hunt, J.C.R. and Fernholz, H., 1975, "Wind-tunnel simulation of the atmospheric boundary layer: a report on Euromech 50", The Journal of Fluid Mechanics, Vol. 70, pp. 543-559. Vol. 7, pp. 361-366.

Larose, G. and D'Auteuil, A. 2006, "On the Reynolds number sensitivity of the aerodynamics of bluff bodies with Sharp edges", Journal of Wind Engineering and Industrial Aerodynamics, Vol. 94, pp. 365-376.

Ligrani, P.M. *et al.*, 1979, "The Thermal and Hydrodynamic Behavior of Thick Rough-Wall Turbulent Boundary Layers", Report No HMT-29, Stanford University.

Ligrani, P.M. *et al.*, 1983, "Artificially Thickened Turbulent Boundary Layers for Studying Heat Transfer and Skin-Friction on Rough Surfaces", Journal of Fluids Engineering, Vol. 105, pp. 146-153.

Loredo-Souza, A.C. *et al.*, 2004, "Simulação da Camada Limite Atmosférica em Túnel de Vento," Turbulência, Vol. 4, pp. 137-160.

Marciotto, E.R. *et al.*, 2012, "Characterization of Surface Level Wind at the Centro de Lançamento de Alcântara for Use in Rocket Structure Loading and Dispersion Studies", Journal of Aerospace Technology and Management, Vol. 4, No. 1, pp. 69-79.

Pires, L.M.B. *et al.*, 2008, "Experimentos em Túnel de Vento da Camada Limite Interna no Centro de Lançamento de Alcântara", Proceedings of Escola de Primavera de Transição e Turbulência, EPTT 2008, São Carlos, São Paulo, Brazil.

Pires, L.B.M., 2009, "Estudo da Camada Limite Interna Desenvolvida em Falésias com Aplicação para o Centro de Lançamento de Alcântara", Tese (Doutorado em Meteorologia), National Institute for Space Research, São José dos Campos, São Paulo, Brazil, 150 p.

Pires, L.B.M. *et al.*, 2010, "Atmospheric Flow Measurements Using the PIV and HWA Techniques", Journal of Aerospace Technology and Management, Vol. 2, No. 2, pp. 127-136.

Wittwer, A. R., *et al.*, 2012, "Avaliação Experimental do Escoamento Atmosférico no Centro de Lançamento de Alcântara Usando Modelos Topográficos em Escala Reduzida", Proceedings of the VIII Escola de Primavera de Transição e Turbulência, 24 a 28 de setembro de 2012, São Paulo – SP, Brazil.